Journal of Zhejiang University-SCIENCE A (Applied Physics & Engineering)
ISSN 1673-565X (Print); ISSN 1862-1775 (Online)
www.jzus.zju.edu.cn; www.springerlink.com
E-mail: jzus@zju.edu.cn

A simple method for calculating in-situ settling velocities of cohesive sediment without fractal dimensions*

Jin-xiao ZHAO†[1], Guo-lu YANG[1], Monika KREITMAIR[2], Yao YUE[1]

[1]*School of Water Resources and Hydropower Engineering, Wuhan University, Wuhan 430071, China*

[2]*School of Engineering, The University of Edinburgh, Edinburgh EH1 1JZ, UK*

†E-mail: jxzhao@nhri.cn

Received Apr. 14, 2017; Revision accepted Oct. 13, 2017; Crosschecked June 6, 2018

Abstract: The settling velocity of sediment flocs is central to the study of the transportation process of contaminants in aqueous ecosystems. To describe the irregular shape of flocs, fractal theory based on the image analysis method is commonly used. However, this method usually leads to non-unique results as it requires the selection of a threshold intensity. Therefore, the main objective of this study is to develop a method to determine the settling velocity of both flocs and particles without using the fractal dimension. To achieve this goal, porosity was introduced as a substitute for the fractal dimension, and a simple method with three variables, floc diameter, mass concentration, and volume concentration of flocs, was developed. A density function method was used to obtain the floc porosity from a laser particle sizer which could obtain the volume concentration of sediment and an optical backscatter point sensor (OBS). Laboratory tests on two sediments from two different lakes were conducted. Results indicate that this method has a higher accuracy than traditional methods such as the Stokes equation and the Rubey equation. The variable density function performed better than the uniform density function and was, therefore, recommended for calculating the settling velocities for both micro and macro flocs. Using the developed method, the drag coefficient for the flocs was calculated and its accuracy analyzed. The method presented in this paper, which is simpler in determining in-situ settling velocities than traditional methods, also allows for direct inter-comparison between results derived from various studies.

Key words: Dredge; Sediment settling; Porosity; In-situ measurement; Density function
https://doi.org/10.1631/jzus.A1700185 **CLC number:** TV81

1 Introduction

The settling velocity of cohesive sediment has significant impact on sediment transport and deposition and contributes substantially to geophysical processes such as the morphodynamics of estuaries, rivers, lakes, and coasts (Spearman et al., 2007; Smith and Friedrichs, 2011), organic carbon and contaminant segregation to deep sea (Boyd and Trull, 2007), and possible contamination caused by suspended sediments in environmental remediation and dredging projects in channels and harbours (Wilber and Clarke, 2001).

One of the most widely used methods to determine this settling velocity is through the use of Stokes equation. However, this method has been shown to be accurate only for impermeable, spherical particles at low Reynolds numbers, that is $Re=\omega d/\upsilon \ll 1$, where ω is the settling velocity of the sediment, d is a characteristic particle size, and υ is the kinematic viscosity of the fluid (Vahedi and Gorczyca, 2012). Cohesive sediments in aquatic environments, however, often

* Project supported by the National Water Pollution Control and Treatment Science and Technology Major Project of China (No. 2014ZX07104-005), the National Natural Science Foundation of China (No. 41601275), and the Fundamental Research Funds for the Central Universities of China (No. 2042015kf0045)

ORCID: Jin-xiao ZHAO, https://orcid.org/0000-0003-3484-8424

settle as large aggregates, known as flocs, as the result of flocculation processes. The morphological characteristics of these flocs are porous and irregular, such that their dynamics depart from those described by Stokes equation (Maggi, 2013). In light of this, to predict the settling velocity of sediment flocs, fractal-based theory has been developed to describe the complex and irregular structure of the aggregates as these may be described mathematically as a fractal system with statistic self-similarity (Meakin, 1991; Kranenburg, 1994).

The most common fractal dimensions used to describe the irregularity of sediment flocs are 2D and 3D. The direct assessment of the dimensionality for 3D fractals is well known to pose significant difficulties and so the majority of 3D fractal dimensions are estimated by using relationships between the 2D and 3D dimensionalities (Maggi, 2008).

A method for the direct measurement of the 3D dimensionality of flocs has been developed by Vahedi and Gorczyca (2011). This method is able to determine the 3D fractal dimension to a high degree of accuracy but cannot be applied in-situ as it requires the use of high precision instruments such as optical microscopes.

Direct assessment of the 2D floc dimension requires optical measurement, for example, through the use of a charge coupled device (CCD) camera, and image processing programs (de Boer et al., 2000). Integral to this method is the choice of an appropriate threshold intensity to convert the 8-bit grey images that are obtained by the camera into binary images to be assessed by the image processing program. Despite being simple in theory, errors are often introduced in the practical application of this process from two main sources:

1. There is no standard procedure for the selection of the threshold intensity and it is commonly selected through algorithms that differ from study to study or trial and error processes (Maggi et al., 2006). This results in non-unique threshold values that can lead to an uncertainty in the fractal dimension, the sediment size, and, ultimately, the settling velocity. As a result, different studies may find different results from the same images.

2. The orientation anisotropy of the shapes, such as the sediment flocs, introduces an error during the calculation of the perimeters and areas of the digitalized images. This results in an "artificial" fractal dimension being obtained, rather than the true dimensionality (Imre, 2006).

Such issues lead to difficulties when applying existing research results to current studies as the error in the calculation of the fractal dimensions prohibits straightforward comparison.

To address these problems, the aim of this study is to develop a simpler method to describe the settling velocity of cohesive sediment without the need of the traditional in-situ fractal dimension measurement. In this method, a physical quantity, namely the porosity, which can be determined uniquely for cohesive sediments, is used as an alternative to fractal dimensions. This then avoids errors introduced by more traditional image processes and provides results that may be more easily compared. In addition, this new method could increase the understanding of floc settling characteristics. This is needed to improve predictive methods commonly used in dredging operation planning and dredged material management.

2 Method

The method developed herein is divided into two parts. The first is a simple equation for calculating the settling velocity of flocs, derived from an equation presented in (Rubey, 1933). The second part calculates the porosity of flocs, based on the mass distribution method (MD-method), as used in (Markussen and Andersen, 2013). These parts will be explored in more detail.

2.1 Settling velocity equation

During the settling process of a floc in a fluid, terminal velocity is reached when there are no net forces acting on the sediment floc, i.e. when gravitational, buoyant, and drag forces are balanced with one another:

$$F_g - F_b = F_v + F_i, \tag{1}$$

where F_g is the force due to gravity, F_b is the force due to the buoyancy of the floc, F_v is the sum of the viscous forces acting on the floc, and F_i is the inertial force.

For sediment flocs, each of these forces may in turn be expressed as follows (Maggi, 2013):

$$F_g = V_f \rho_f g = a d_f^3 \rho_f g, \tag{2a}$$

$$F_b = V_f \rho_w g = a d_f^3 \rho_w g, \tag{2b}$$

$$F_v = 4 P_f \mu \omega = c (b d_f^2)^{\frac{9}{16D}+\frac{7}{16}} \mu \omega, \tag{2c}$$

$$F_i = A_f \rho_f \omega^2 = b d_f^2 \rho_f \omega^2, \tag{2d}$$

where d_f is the diameter of sediment flocs, ρ_w and ρ_f are the densities of fluid and sediment flocs, respectively, g is the gravitational acceleration, μ is the viscosity of fluid, and ω is the settling velocity. V_f, A_f, and P_f are the volume, projected area, and perimeter of the sediment flocs, respectively. The parameters a, b, and c are form factors that relate to the floc. Thus, a relationship between the fractal dimension, D, and the porosity can be found, and a new settling equation may be derived without the explicit use of the fractal dimension.

For a single floc, assuming that the size of primary particles within the floc is constant, the following expressions are obtained for the volumes of particles and flocs:

$$(1-e)V_f = NV_p, \tag{3a}$$

$$V_f = \frac{1}{6}\pi d_f^3, \tag{3b}$$

$$V_p = \frac{1}{6}\pi d_p^3, \tag{3c}$$

where e is the porosity of the floc and N is the number of primary particles in the floc, d_p is the diameter of primary particles, and V_p is the volume of primary particles in the floc.

By substituting the expressions for the volumes, Eqs. (3b) and (3c), into Eq. (3a), an expression for N in terms of the floc and primary particle diameters and the porosity is obtained:

$$N = (1-e)(d_f / d_p)^3 = (1-e) l^3, \tag{4}$$

where $l=d_f/d_p$.

According to fractal theory, $N=l^D$ (Falconer, 1990), a relationship between porosity and fractal dimension may be derived:

$$D = \log_l (1-e) + 3. \tag{5}$$

Consequently, the value of the fractal dimension of the floc is equal to 3 when the porosity of the floc is 0, as is to be expected for a solid floc without any porosity.

The substitution of Eq. (5) into Eq. (2c) and the use of Eqs. (2a)–(2d) in the force balance, Eq. (1), yield a quadratic equation in the settling velocity, ω. Solving this, the expression obtained is

$$\omega = \left[-3c\mu (b d_f^2)^{E/2} + \sqrt{9c^2\mu^4 (b d_f^2)^E + 4ab\rho_f g(\rho_f - \rho_w) d_f^5} \right] \Big/ (2b\rho_f d_f^2), \tag{6}$$

where the form factor E is given by

$$E = \frac{9}{8[\log_l (1-e) + 3]^2} + \frac{7}{8}.$$

For single particles, the form factors a, b, and c are given by $a=\pi/6$, $b=\pi/4$, and $c=2\pi^{0.5}$, and the porosity is $e=0$. These substitutions reduce Eq. (6) to the Rubey equation (Rubey, 1933).

The same form factors apply for flocs, thereby introducing approximations to V_f, A_f, and P_f, and are within the acceptable tolerance levels as given in (Maggi, 2013). In the following text, Eq. (6) is referred to as the "NF equation" for convenience, underlining the absence of a fractal dimension ("NF" stands for "non-fractal").

2.2 Method to determine floc porosity

Previous study shows that there exists a relationship between floc porosity and density (Fettweis, 2008). Under the assumption that all pores in the flocs are filled with water, this relation may be expressed as

$$e = \frac{\rho_p - \rho_f}{\rho_p - \rho_w}, \tag{7}$$

where ρ denotes the density, and the subscripts w, p, and f denote water, primary particles, and flocs, respectively. The densities of primary particles and of water are easily obtained, such that the porosity of the

flocs can be calculated as long as the density of flocs, ρ_f, is known. To calculate ρ_f, Markussen and Andersen (2013) proposed an MD-method, whereby floc density and floc size are related via a power law of the form:

$$\rho_f = \varepsilon d_f^{\delta}, \tag{8}$$

where ε and δ are appropriately chosen constants (Dyer and Manning, 1999; Mikkelsen and Pejrup, 2000). To solve for these constants, four either known or estimated parameters are required: (1) the size d_p and density ρ_p of the primary sediment, and (2) the mean size d_{fm} and mean density ρ_{fm} of floc.

For the first of these two parameters, the diameter of primary sediment d_p can be measured directly through the use of a laser particle sizer. The density of the primary sediment ρ_p may be determined through a loss of ignition (LOI) test, as sediments collected from Guanqiao (GQ) and Moshui (MS) lakes consist of organic matter and inorganic mineral. Using this method, the density is given by $\rho_p=(1-L)\rho_i+L\rho_o$, where L is the ignition loss, ρ_o is the density of organic matter that was assumed to be 1300 kg/m^3, and ρ_i is the density of inorganic mineral which was taken to be 2650 kg/m^3 (Markussen and Andersen, 2013).

For the second condition, the mean diameter of floc d_{fm} may also be measured by a laser particle sizer, such as LISST devices. The mean floc density is calculated using the equation $\rho_{fm}=M_{fc}/V_{fc}$ in which V_{fc} is measured by a LISST device and M_{fc} is calculated from the properties of the water, primary particles, and flocs via

$$\begin{aligned} M_{fc} &= M_{pc} + M_{wc} = M_{pc} + \rho_w (V_{fc} - V_{pc}) \\ &= M_{pc} + \rho_w \left(V_{fc} - \frac{M_{pc}}{\rho_p} \right), \end{aligned} \tag{9}$$

where M_{wc}, M_{pc}, and M_{fc} are the mass concentrations of water, primary particles, and flocs, respectively, and V_{wc}, V_{pc}, and V_{fc} are the volume concentrations of water, primary particles, and flocs, respectively (Kranenburg, 1994; Voulgaris and Meyers, 2004). M_{pc} was obtained by an optical backscatter point sensor (OBS).

With d_p, ρ_p and d_{fm}, ρ_{fm} determined, the constants ε and δ in Eq. (8) may then be calculated using the expressions (Falconer, 1990):

$$\varepsilon = \frac{\log\left(\rho_{fm}/\rho_p\right)}{\log\left(d_{fm}/d_p\right)}, \quad \delta = \frac{\rho_p}{d_p^{\varepsilon}}. \tag{10}$$

For particles of diameter smaller than d_p the density is set equal to ρ_p, while for larger particles the density is calculated using the density law given in Eq. (8). As the floc density is known, the porosity of the floc can be obtained from Eq. (7).

There now remain three undefined parameters in the NF equation: d_f, e, and ρ_f. However, both the porosity and the floc density are functions of the floc diameter, as given by Eqs. (7) and (8) leaving only one unknown, namely the size of flocs. This makes it unlike other sediment flocculation settling velocity formulas, as it does not use any fractal dimensions.

3 Experimental

The accuracy of the proposed method was tested by comparison of the calculated settling velocities with experimentally determined values. To this end, a sediment settling velocity measurement system (SSVMS) was used, consisting of a purpose-built sediment sampler, a particle imaging camera system (PICS), an OBS, and a Sequoia LISST-100c (Agrawal and Pottsmith, 2000). These experimental components are now explained in more detail.

3.1 Sediment sampler

The sediment sampler consisted of a rectangular settling column, of dimensions 5 cm×5 cm×60 cm, made of plexiglass (Fig. 1). The two ends of the sampler were blocked to allow for the device to be reversed, i.e. turned up-side-down, while two openings and a vent pipe were placed at one side, each opening fitted with a control valve. The sampler was then used as a settling volume during subsequent measurements.

3.2 Particle imaging camera system

The PICS consisted of a CCD camera and a light-emitting diode (LED) lighting system and was

used to measure flocs size and settling velocity. A Manta G-201B CCD camera (AVT, Germany) was used to measure the image data of sediment flocs. This CCD camera was a fast GigE Vision camera with a Sony ICX274 sensor. It ran at 30 frame/s with a full resolution of 1624×1234, giving a pixel size of 4.54 μm, smaller than the mean size of primary sediment particles. This camera was placed 10 mm above the bottom of sampler giving a settling distance of 50 mm, which was long enough to ensure that the terminal settling velocity had been reached by the sediment flocs (Shang et al., 2014). Two LED lights were aligned orthogonally to the line of sight of the CCD camera to illuminate the sediment (Fig. 1).

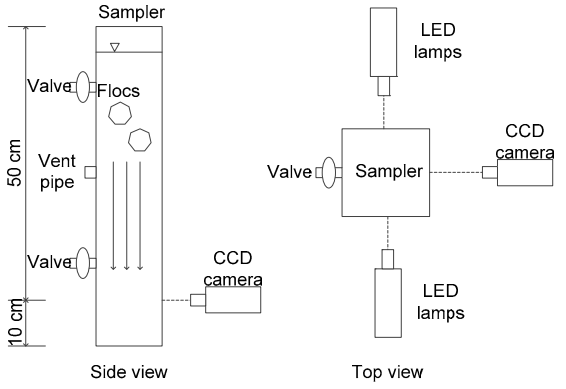

Fig. 1 Top and side views of the purpose-built sampler when it is used as settling volume in PICS

3.3 LISST and OBS sensor

The LISST is a laser particle analyzer, capable of obtaining the in-situ particle size distribution without disturbing the flocs and leading them to break up. The LISST uses laser diffraction to measure the particle size distributions in 32 logarithmically spaced size classes over the range 5–500 μm. The LISST was mainly used to measure the volume concentration and mean size of the sediment sample. Similarly, the OBS senor was able to obtain the in-situ mass concentration of sediment sample without disturbance.

3.4 Experimental methodology

The in-situ measurement of cohesive sediment presents challenges as the experimental parameters and sampling sediments are difficult to control. To this end, a 5 m×1 m×2.5 m (length×width×depth) tank was constructed to simulate field conditions. Sediment was collected from two locations in the city of Wuhan, China: (1) the Moshui lake in the west (designated as MS data) and (2) the Guanqiao lake in the east (GQ data). These sites had been chosen as both had been previously subjected to severe pollution and dredging by the local government.

The testing tank was prepared by distributing a homogenous, 0.5 m thick layer of the contaminated sediment throughout the tank, over an aeration device. This device was used to suspend the upper sediment into the 1.5 m lake-water layer that was filled into the tank. Measurements were taken at a depth of 0.5 m from the surface of the water.

The aeration intensity was calibrated to ensure optimal sediment concentration at the point of measurement. Too high a concentration prohibited subsequent image analysis while too low reduced the efficiency of the test. The optimal range for the sediment concentration was found to be 0.5−1.0 g/L (Furukawa et al., 1997; Delnoij et al., 1999; Callens et al., 2008). A schematic of the experimental setup is shown in Fig. 2.

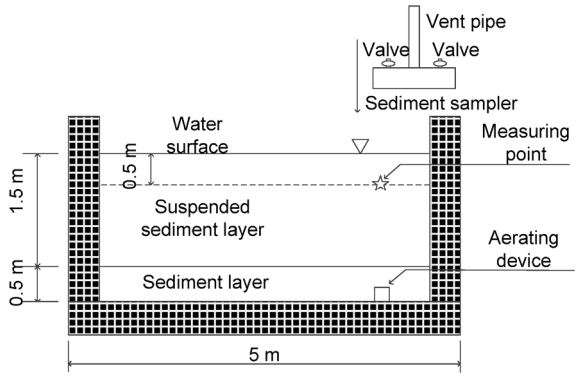

Fig. 2 Experimental set-up of sediment tank

Before each experiment was started, the OBS device needed to be calibrated. First, the aeration device was opened and sediment was suspended in the water layer. After that, sediments from different depths were sampled while the turbidity at each depth was also measured by the OBS device. All sampling points were sited in a vertical line and each measurement lasted for 20–30 s. The mass concentration of those sediment samples was measured by stoving and weighing. Finally, the OBS device was calibrated

based on those results of mass concentration and corresponding turbidity.

At the beginning of the experiment, sediment was suspended in the water layer using the aerating apparatus. The LISST and OBS devices were placed at the measuring point to monitor the sediment concentration in real time. When the concentration of sediment was stabilized and within the predetermined range, the sampler was lowered to the measuring point with both valves closed. The valves were then opened to allow the surrounding fluid into the sampler. Simultaneously, sediment volume and mass concentration data were collected to ensure correct correspondence with the settling volume and to subsequently determine the density function.

3.5 Measurement of sediment size and settling velocity

Upon completion of the sample collection, the sampler was extracted from the tank and the settling of the flocs within it was recorded using the CCD camera. This process had to be completed swiftly to be able to make the assumption that the flocs had not been broken and the data collected by the LISST and OBS devices were appropriate for determining the power law describing the floc density within the sampler.

The camera's inbuilt program was able to monitor the image of flocs in real time. When the settling of sediment had reached terminal velocity, the 30 frame/s video was recorded until the majority of sediment had settled to the bottom. The sampler was then reversed to continue the measurement.

An image processing program was developed to analyze the size and settling velocity of the sediment. In the program the focus was on only one sediment floc in a loop. The threshold value of the grey image recorded was selected by trial and error. Eleven consecutive frames were used to calculate 10 groups of sediment size and velocity on the vertical and horizontal directions respectively. The average of sizes was used as the floc size and similarly the average of velocities on the vertical direction was recognized as the terminal settling velocity. Considering that the observed sediment flocs in this study were in a state of uniform motion, there should not be many differences between these calculated floc sizes and velocities in the vertical direction. In addition, as the aim of this method was to predict the settling velocity in still water, the velocities on the horizontal direction should be within a tolerance range. Therefore, the variance of calculated floc sizes and velocities in the vertical direction and the average of absolute values of velocities on the horizontal direction were also calculated in a loop.

If any of these three results were beyond the pre-set limit, the result for this floc was not used. The selection of flocs in this program is manual and random, but it is also based on some principles such as that the image of the floc should be clear and not overlapped with other flocs during the settling process.

4 Results

Both Stokes' law and the Rubey equation have been shown to introduce errors in cases in which the Reynolds numbers are too high (Brinke, 1994). As the Reynolds number increases with floc diameter, datasets were classified into one of two types depending on the floc diameter so as to study the effect of sediment size on the performance of the developed method. Sediments with a diameter smaller than 62 μm were categorized as micro sediments and those with a diameter greater than 62 μm as macro sediments. This size threshold is equivalent to the standard distinction between silt and sand (Zhang, 1998).

4.1 Sediment characteristics

To calculate the parameters for the power law to describe the effective floc density, Eq. (8), sediment characteristics for the two lake samples needed to be acquired, as described in Section 2.2. The determination of these characteristics is outlined below and summarized in Table 1.

Prior to the experiment, portions of the lake samples were filtered and dispersed to determine both the mean diameter of primary particles, d_p, using a laser particle size analyzer Mastersizer 2000 (Sochan et al., 2012), and the LOI via a muffle furnace. At the start of the experiment, simultaneous measurements of the volume concentration, V_{fc}, and the mean

diameter, d_{fm}, of the sediment flocs were performed at the measurement point using the LISST device. These were then used to determine the density function for the flocs.

4.2 Power law of the effective density of flocs

Using Eqs. (8) and (10) together with the data of Table 1, the effective density functions for the sediment samples from the two lakes were determined. The effective density is defined as ($\rho_f - \rho_w$). Fig. 3 shows a plot of these, alongside effective density functions obtained in previous studies. The power laws for the GQ and MS lakes show good agreement with these studies.

Table 1 Characteristics of cohesive sediment collected from both lakes

Parameter	Value	
	MS data	GQ data
Mean diameter of primary particles, d_p (μm)	9.23	6.11
Mean diameter of flocs, d_{fm} (μm)	100.12	92.94
Density of primary particles, ρ_p (kg/m^3)	2542	2455
Density of sediment flocs, ρ_{fm} (kg/m^3)	1180	1190
Loss on ignition, LOI (%)	8	7

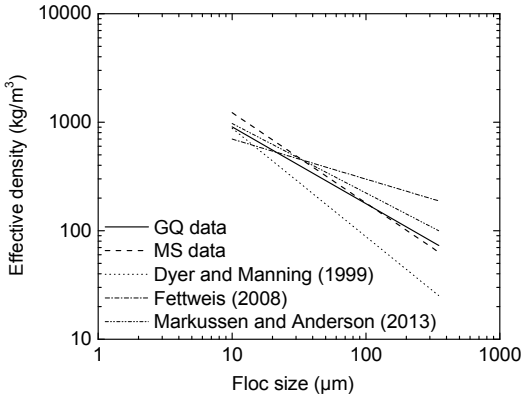

Fig. 3 Power law of floc effective density against floc size shown alongside previous studies

4.3 Settling velocity

To test the method presented in this study, the settling velocity of sediment flocs was determined experimentally for each of the two lake sediment samples. In each measurement, the settling volume was turned over at most twice to prevent floc-breaking. The total time of video recorded in each run was about 30 min and the developed image process program was applied to analyze these videos.

The recorded floc sizes ranged between 20 and 400 μm and settling velocities varied between 0.0001 and 0.01 m/s. These both fell in the range of previous studies (Sumer et al., 1996; Agrawal and Pottsmith, 2000; Voulgaris and Meyers, 2004).

To test the precision of the calculation of settling velocity, the NF equation was compared with Stokes equation, which assumes a drag coefficient of C_d=24/*Re*, and the original Rubey equation, respectively given by

$$\omega = \frac{g}{18\mu}(\rho_f - \rho_w)d_f^2, \tag{11}$$

$$\omega = \frac{-18\mu + \sqrt{18^2\mu^2 + 6gd_f^3\rho_f(\rho_f - \rho_w)}}{3d_f\rho_f}. \tag{12}$$

In many cases the effective density of flocs was not known and a single effective density was used instead (Maggi, 2013). To determine the effect of the chosen density on the calculation of the settling velocity, the values obtained from using either a density power law function or a uniform density were compared. The results for this are shown in Fig. 4 and are discussed in the next section.

4.4 Goodness of fit

The correlation coefficient *R* and the normalized root mean square error (NRMSE) were used to assess the "goodness of fit" of the methods used. These parameters are defined as:

$$\mathrm{NRMSE} = \frac{\sqrt{\frac{1}{n}\sum(M-O)^2}}{\overline{O}}, \tag{13}$$

$$R = \frac{\mathrm{Cov}(M,O)}{\sqrt{D(M)}\sqrt{D(O)}} = \frac{\sum(M-\overline{M})(O-\overline{O})}{\sqrt{\sum(M-\overline{M})^2}\sqrt{\sum(O-\overline{O})^2}}, \tag{14}$$

where M and O denote modelled and observed settling velocities, respectively, $D(\cdot)$ is the variance, and n is the number of data.

Tables 2 and 3 give a comparison of the correlation coefficient R and NRMSE of the three different equations for each of the two methods to determine density, for both micro and macro flocs.

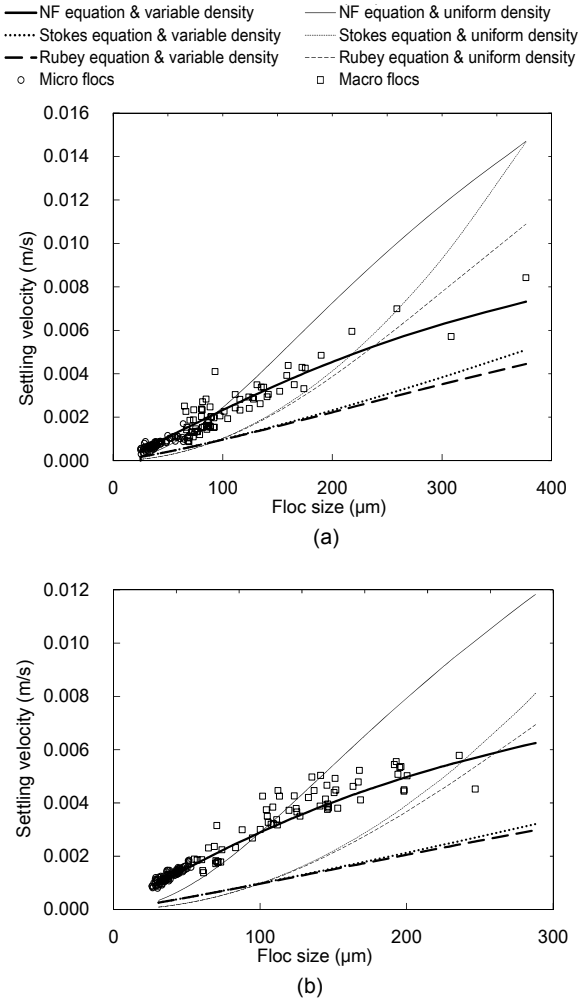

Fig. 4 Observed and modelled settling velocities versus floc size for the GQ lake sediment samples (a) and MS lake sediment samples (b)

5 Discussion

5.1 Comparison between various equations with a given density method

The modelled results of the six different approaches (three equations with the two density methods applied to each) and the observed data are shown in Fig. 4 to compare the accuracy of the methods. In general, very good agreement is achieved with experimental data by the combination of the NF equation with the density power law (the thick solid line). It is the only one of the six modelled approaches that exhibits a flattening of the slope at higher floc sizes, consistent with the observed behaviour.

Table 2 Correlation coefficient R for the three methods used to determine the settling velocities of sediment flocs

Density method	Equation	Correlation coefficient R			
		GQ data		MS data	
		Micro floc	Macro floc	Micro floc	Macro floc
Variable density	Stokes equation	0.87	0.85	0.89	0.87
	Rubey equation	0.89	0.82	0.89	0.88
	NF equation	0.92	0.88	0.90	0.89
Uniform density	Stokes equation	0.86	0.84	0.89	0.80
	Rubey equation	0.89	0.84	0.89	0.83
	NF equation	0.84	0.92	0.89	0.89

Table 3 NRMSE for the three methods used to determine the settling velocities of sediment flocs

Density method	Equation	NRMSE			
		GQ data		MS data	
		Micro floc	Macro floc	Micro floc	Macro floc
Variable density	Stokes equation	0.61	0.62	0.69	0.62
	Rubey equation	0.61	0.64	0.70	0.64
	NF equation	0.19	0.22	0.20	0.23
Uniform density	Stokes equation	0.79	0.59	0.85	0.45
	Rubey equation	0.79	0.51	0.85	0.45
	NF equation	0.41	0.57	0.45	0.66

Comparison of different equations for a given density method shows that the velocities obtained from the NF equation (solid line) are consistently

higher than those obtained from either Stokes equation or Rubey equation, irrespective of the density method used. The introduction of sediment porosity in the NF equation decreases the drag forces on the floc whilst gravity and buoyancy forces remain unaffected. Equilibrium is therefore reached at a higher settling velocity, necessary to achieve sufficient drag. Furthermore, the velocities obtained from Stokes equation and Rubey equation are very similar for micro flocs, but diverge as the floc size increases, with Stokes equation giving a higher velocity. Stokes equation does not take into consideration the inertial forces when determining the settling velocities of the sediment aggregates. However, with increasing floc size these forces become increasingly less negligible, despite inertial forces not playing a primary role in the drag forces.

Comparison of the three equations shows no significant differences in the correlation coefficients, neither between the uniform density and the variable density methods. Of note is the improved performance of the NF equation over Stokes equation and the Rubey equation for data from both lakes, with increased values for R by an average of 0.035 for micro and 0.075 for macro flocs. Furthermore, for a given method of determining the settling velocity using a given density method, the correlation coefficients for macro flocs were lower than those for micro flocs, indicating that all three methodologies performed to a higher accuracy for sediment flocs of smaller diameter.

Analysis of the NRMSE values showed a general improvement in the accuracy of the determined settling velocities when using the newly developed method. For the variable density method proposed in this study, the NRMSE was found to be lower using the NF equation with an average of 0.21 than for either of the other two methods. Overall, the use of the NF equation combined with the variable density gave the lowest NRMSE values. The errors found for Stokes equation and the Rubey equation were very similar for a given density function and floc size.

5.2 Comparison of the density methods

Comparison of plots of the same equations but with different density methods in Fig. 4 allows the effect of the density on the calculated settling velocities to be analyzed. The relative difference (RD= $|V_{DF}-V_{UD}|/V_{DF}$) and the absolute difference (AD= $|V_{DF}-V_{UD}|$) between the settling velocities calculated from the uniform density and the variable density methods have also been calculated and are shown in Fig. 5, where V_{DF} and V_{UD} are settling velocities of density function and uniform density method, respectively.

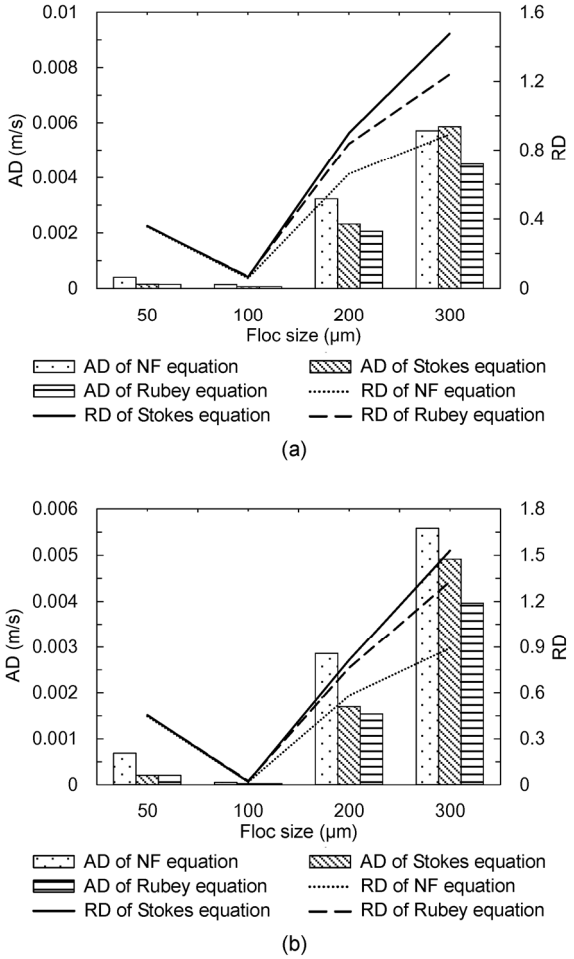

Fig. 5 RD and AD of GQ (a) and MS (b) data for different equations versus floc size

Comparing the plots of the same equations but with different density methods in Fig. 4, differences of settling velocity between variable density and uniform density methods appeared as a decrease as floc size increased, and then a decelerated growth appeared until the flocs size reached over 300 μm. An intersection point of these two different density

methods, where density determined by the density function equals the uniform density, were found. This trend can also be seen in AD (histogram) and RD (lines) for a given equation in Fig. 5.

For flocs smaller than those at the intersection point, comparison of the three equations shows no significant differences in the relative velocity difference. As floc size increased, the NF equation exhibited the smallest relative difference from the three approaches. This implies that the new equation is the least sensitive to the choice in density method used in the calculation of settling velocity of macro flocs. However, the RD of the NF equation still reached 100% when the floc size increased to 300 μm. In other words, the settling velocity of uniform density almost doubled when using the variable density method.

As may be seen from the goodness of fit values in Tables 2 and 3, the NF equation combined with the variable density method has a higher accuracy than combination with the uniform density, regardless of floc size. However, the results from the Stokes equation and the Rubey equation differed greatly between the two density methods. For these two equations, the variable density calculation performed better than the uniform density for micro flocs, but worse for macro flocs. Because of this, it should not be concluded that the variable density method, which assumes that the density of the flocs decreases as the sediment size grows, was more consistent with the practical situation than uniform density method. The reason why uniform density method had a better performance on macro flocs is that the Stokes equation and the Rubey equation were not suitable for flocs. Errors caused by density and relation of drag forces in these two equations were counteracting each other to a certain extent in this situation.

5.3 Analysis of drag coefficients

Traditionally, the settling of sediment flocs is characterized into different regimes based on the value of the Reynolds number of the system. In each regime, the relation of drag coefficients C_d was also different. Jiang and Logan (1991) proposed a power law relationship between Reynolds number and drag coefficients for particles when Re is not in the creeping flow region (the Reynolds number for creeping flow is $Re \ll 1$). The drag coefficient is given by

$$C_d = \gamma Re^{-\eta}. \tag{15}$$

In the study, for $Re \ll 1$, the constants were determined to be γ=24 and η=1, from which the Stokes equation can be derived. For the transition region of $0.1<Re<10$, the constants were γ=29.03 and η=0.871.

Using the power law of Eq. (15), values for the parameters γ and η were determined empirically from the observed settling velocities, and are plotted in Fig. 6. For GQ lake data, the constants were found to be γ=10.16 and η=0.91, while for the MS lake data they were determined to be γ=9.62 and η=0.81. Compared with the study of Jiang and Logan (1991), the γ constant was far smaller and the index η was almost the same.

Fig. 7 shows the relationship between sediment size and Reynolds number in both lake datasets. Square dots represent MS data and circular dots

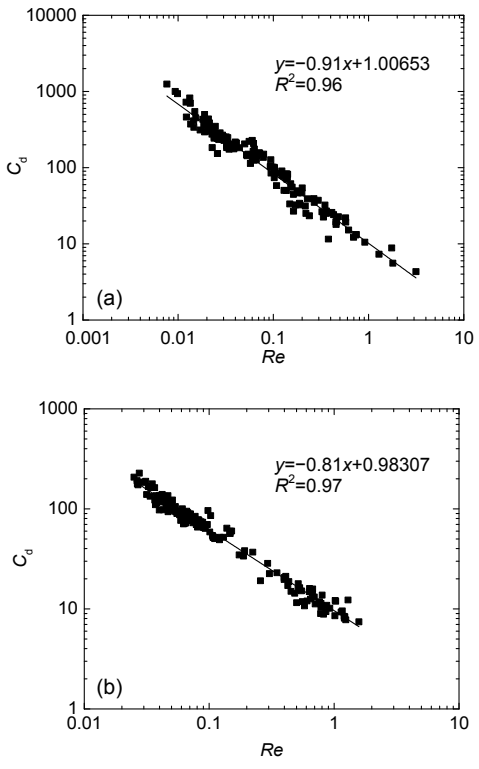

Fig. 6 Relations between Re and C_d for GQ (a) and MS (b) data

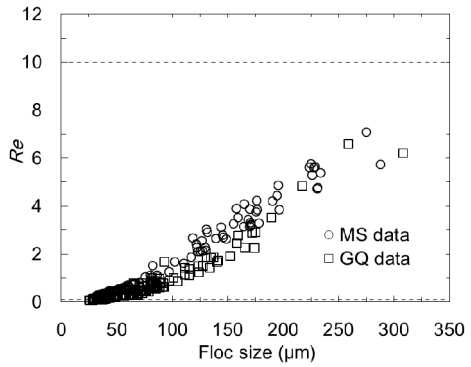

Fig. 7 *Re* of sediment flocs versus different floc sizes

represent GQ data. Dashed lines represent the upper and lower limits of settling regime with a *Re* range from 0.1 to 10. The majority of flocs fell into the regime in which $0.1<Re<10$. This illustrates that the η index, defined by Eq. (15), was predominantly determined by the flow regime rather than the structure of flocs. The fact that the sediment studied in this paper is very different to that studied by Jiang and Logan (1991) implies that the γ constant, on the other hand, is influenced mainly by sediment properties.

6 Conclusions

In this paper, a simple method was developed to predict the in-situ terminal velocity of cohesive sediment flocs. This method consists of two major parts: a newly developed settling equation in which the porosity is used as a replacement for the traditional fractal dimension and a method to calculate the porosity of sediment flocs, based on a density function. The developed method is very simple as the equation used contains three unknown variables, the floc size, the mass concentration, and the volume concentration of flocs. It therefore avoids errors introduced by the non-uniqueness of fractal dimensions as is common with traditional methods and the results obtained by this method agree well with those found in previous studies.

The method developed herein alongside two established equations has been tested using two experimental datasets. Results indicate that the proposed method exhibits an improved accuracy in the calculation of settling velocity as compared with both the Stokes equation and the Rubey equation. Furthermore, a comparison between a variable density method and a uniform density method revealed that the former was more consistent with the density distribution of flocs and is thus recommended for the calculation of settling velocities. Finally, the constants in determining drag coefficients were analyzed, with the result that the η index defined was mainly determined by the flow regime while the constant γ was influenced by the sediment properties.

It should be noted that the settling velocity in the new method is determined by one single parameter of floc size according to NF equation as long as the density function of flocs is obtained. However, macro flocs of the same size can have different settling velocities which distribute randomly. Therefore, further study is still needed to improve the method presented in this paper.

References

Agrawal YC, Pottsmith HC, 2000. Instruments for particle size and settling velocity observations in sediment transport. *Marine Geology*, 168(1-4):89-114. https://doi.org/10.1016/S0025-3227(00)00044-X

Boyd PW, Trull TW, 2007. Understanding the export of biogenic particles in oceanic waters: is there consensus? *Progress in Oceanography*, 72(4):276-312. https://doi.org/10.1016/j.pocean.2006.10.007

Brinke WBMT, 1994. Settling velocities of mud aggregates in the Oosterschelde tidal basin (the Netherlands), determined by a submersible video system. *Estuarine, Coastal and Shelf Science*, 39(6):549-564. https://doi.org/10.1016/S0272-7714(06)80009-0

Callens N, Minetti C, Coupier G, et al., 2008. Hydrodynamic lift of vesicles under shear flow in microgravity. *EPL (Europhysics Letters)*, 83(2):24002. https://doi.org/10.1209/0295-5075/83/24002

de Boer DH, Stone M, Levesque LM, 2000. Fractal dimensions of individual flocs and floc populations in streams. *Hydrological Processes*, 14(4):653-667. https://doi.org/10.1002/(SICI)1099-1085(200003)14:4<653::AID-HYP964>3.0.CO;2-3

Delnoij E, Westerweel J, Deen NG, et al., 1999. Ensemble correlation PIV applied to bubble plumes rising in a bubble column. *Chemical Engineering Science*, 54(21):5159-5171. https://doi.org/10.1016/S0009-2509(99)00233-X

Dyer KR, Manning AJ, 1999. Observation of the size, settling velocity and effective density of flocs, and their fractal

dimensions. *Journal of Sea Research*, 41(1-2):87-95. https://doi.org/10.1016/S1385-1101(98)00036-7

Falconer KJ, 1990. Fractal Geometry Mathematical Foundations and Applications. John Wiley & Sons, Hoboken, USA, p.499-500.

Fettweis M, 2008. Uncertainty of excess density and settling velocity of mud flocs derived from in situ measurements. *Estuarine, Coastal and Shelf Science*, 78(2):426-436. https://doi.org/10.1016/j.ecss.2008.01.007

Furukawa K, Wolanski E, Mueller H, 1997. Currents and sediment transport in mangrove forests. *Estuarine, Coastal and Shelf Science*, 44(3):301-310. https://doi.org/10.1006/ecss.1996.0120

Imre AR, 2006. Artificial fractal dimension obtained by using perimeter–area relationship on digitalized images. *Applied Mathematics and Computation*, 173(1):443-449. https://doi.org/10.1016/j.amc.2005.04.042

Jiang Q, Logan BE, 1991. Fractal dimensions of aggregates determined from steady-state size distributions. *Environmental Science & Technology*, 25(12):2031-2038. https://doi.org/10.1021/es00024a007

Kranenburg C, 1994. The fractal structure of cohesive sediment aggregates. *Estuarine, Coastal and Shelf Science*, 39(6):451-460. https://doi.org/10.1016/S0272-7714(06)80002-8

Maggi F, 2008. Projection of compact fractal sets: application to diffusion-limited and cluster-cluster aggregates. *Nonlinear Processes in Geophysics*, 15(4):695-699. https://doi.org/10.5194/npg-15-695-2008

Maggi F, 2013. The settling velocity of mineral, biomineral, and biological particles and aggregates in water. *Journal of Geophysical Research: Oceans*, 118(4):2118-2132. https://doi.org/10.1002/jgrc.20086

Maggi F, Manning AJ, Winterwerp JC, 2006. Image separation and geometric characterisation of mud flocs. *Journal of Hydrology*, 326(1-4):325-348. https://doi.org/10.1016/j.jhydrol.2005.11.005

Markussen TN, Andersen TJ, 2013. A simple method for calculating in situ floc settling velocities based on effective density functions. *Marine Geology*, 344(4):10-18. https://doi.org/10.1016/j.margeo.2013.07.002

Meakin P, 1991. Fractal aggregates in geophysics. *Reviews of Geophysics*, 29(3):317-354. https://doi.org/10.1029/91RG00688

Mikkelsen OA, Pejrup M, 2000. In situ particle size spectra and density of particle aggregates in a dredging plume. *Marine Geology*, 170(3-4):443-459. https://doi.org/10.1016/S0025-3227(00)00105-5

Rubey WW, 1933. Settling velocity of gravel, sand, and silt particles. *American Journal of Science*, s5-25(148):325-338. https://doi.org/10.2475/ajs.s5-25.148.325

Shang QQ, Fang HW, Zhao HM, et al., 2014. Biofilm effects on size gradation, drag coefficient and settling velocity of sediment particles. *International Journal of Sediment Research*, 29(4):471-480. https://doi.org/10.1016/S1001-6279(14)60060-3

Smith SJ, Friedrichs CT, 2011. Size and settling velocities of cohesive flocs and suspended sediment aggregates in a trailing suction hopper dredge plume. *Continental Shelf Research*, 31(10):S50-S63. https://doi.org/10.1016/j.csr.2010.04.002

Sochan A, Bieganowski A, Ryżak M, et al., 2012. Comparison of soil texture determined by two dispersion units of Mastersizer 2000. *International Agrophysics*, 26(1):99-102. https://doi.org/10.2478/v10247-012-0015-9

Spearman J, Bray RN, Land J, et al., 2007. Plume dispersion modelling using dynamic representation of trailer dredger source terms. *Proceedings in Marine Science*, 8:417-448. https://doi.org/10.1016/S1568-2692(07)80025-8

Sumer BM, Kozakiewicz A, Fredsøe J, et al., 1996. Velocity and concentration profiles in sheet-flow layer of movable bed. *Journal of Hydraulic Engineering*, 122(10):549-558. https://doi.org/10.1061/(asce)0733-9429(1996)122:10(549)

Vahedi A, Gorczyca B, 2011. Application of fractal dimensions to study the structure of flocs formed in lime softening process. *Water Research*, 45(2):545-556. https://doi.org/10.1016/j.watres.2010.09.014

Vahedi A, Gorczyca B, 2012. Predicting the settling velocity of flocs formed in water treatment using multiple fractal dimensions. *Water Research*, 46(13):4188-4194. https://doi.org/10.1016/j.watres.2012.04.031

Voulgaris G, Meyers ST, 2004. Temporal variability of hydrodynamics, sediment concentration and sediment settling velocity in a tidal creek. *Continental Shelf Research*, 24(15):1659-1683. https://doi.org/10.1016/j.csr.2004.05.006

Wilber D, Clarke D, 2001. Biological effects of suspended sediments: a review of suspended sediment impacts on fish and shellfish with relation to dredging activities in estuaries. *North American Journal of Fisheries Management*, 21(4):855-875. https://doi.org/10.1577/1548-8675(2001)021<0855:BEOSSA>2.0.CO;2

Zhang RJ, 1998. River Sediment Dynamics. China Water Power Press, Beijing, China, p.35-36 (in Chinese).

中文概要

题　目：不含分形维数的细颗粒泥沙沉速计算方法研究

目　的：推导一种高精度、使用简单且不含有分形维数的细颗粒泥沙沉速计算方法，以应用于原位观测和

实现不同计算结果间的相互比较。

创新点： 1. 推导出了不含有分形维数的泥沙絮团沉速公式；2. 将 LISST 等高精度仪器应用于泥沙絮团密度计算中。

方　法： 1. 通过理论推导，得到不含分形维数的粘性细颗粒泥沙沉速公式；2. 通过试验对该公式的精度进行研究，并在此基础上研究不同密度计算方法对该公式精度的影响；3. 研究不同沉速状态下，泥沙絮团的沉降规律。

结　论： 1. 通过对比实测沉速与计算沉速的结果可以看出，本文提出的絮团沉速公式在计算泥沙絮团的沉速时精度较高；2. 通过比较两种不同密度计算方法的结果可以看出，变密度方法具有更高的精度；3. 通过拟合结果可以看出，公式（15）中的参数 η 与泥沙所处的沉降区间有关，参数 γ 与泥沙自身的性质有关。

关键词： 疏浚；泥沙沉速；孔隙率；原位观测；密度函数